International Journal of Electrical, Electronic and Communication Sciences
ISSN: 2517-9438
Vol:7, No:9, 2013

Optimal current control of externally excited synchronous machines in automotive traction drive applications

Oliver Haala, Bernhard Wagner, Maximilian Hofmann and Martin März

Abstract—The excellent suitability of the externally excited synchronous machine (EESM) in automotive traction drive applications is justified by its high efficiency over the whole operation range and the high availability of materials. Usually, maximum efficiency is obtained by modelling each single loss and minimizing the sum of all losses. As a result, the quality of the optimization highly depends on the precision of the model. Moreover, it requires accurate knowledge of the saturation dependent machine inductances. Therefore, the present contribution proposes a method to minimize the overall losses of a salient pole EESM and its inverter in steady state operation based on measurement data only. Since this method does not require any manufacturer data, it is well suited for an automated measurement data evaluation and inverter parametrization. The field oriented control (FOC) of an EESM provides three current components resp. three degrees of freedom (DOF). An analytic minimization of the copper losses in the stator and the rotor (assuming constant inductances) is performed and serves as a first approximation of how to choose the optimal current reference values. After a numeric offline minimization of the overall losses based on measurement data the results are compared to a control strategy that satisfies $\cos(\varphi) = 1$.

Keywords—Current control, efficiency, externally excited synchronous machine, optimization.

I. Introduction

DURING the last years the EESM registered an increase in the market for electric vehicles [1]. This is due to the high efficiency over the whole operation range, the high torque at startup and the high availability of necessary materials. Moreover, the excitation current represents an additional degree of freedom (DOF) which allows to meet safety requirements comfortably [2] and is useful for the rotor position estimation ([3], [4]) so that the resolver might become obsolete in future applications.

However, this additional DOF needs to be considered in the torque control. In each operating point there is (at least) one excitation current that is optimal in terms of an efficiency maximization. If there is a high demand for the dynamic behaviour, however, due to a comparatively high rotor time constant it is necessary to provide a minimum excitation current at any time. Moreover, since the rotor is usually not actively cooled, the rotor temperature needs to be considered. This contribution focuses on the determination of the optimal excitation current but it also provides a strategy to adapt the stator current components if the excitation current is above or below its optimal value.

The minimization of the motor losses is analysed in [5] and [2]. For this purpose the motor is modelled by a finite element method. A high motor efficiency is obtained by modelling each single loss and minimizing the sum of all losses. In [5] the sum of the copper losses and the iron losses are considered, whereas [2] considers the stray losses additionally. However, since these methods are based on a finite element analysis, the full knowledge of all machine geometries and materials is required. Moreover, the stray losses are difficult to model because the causes are diverse [7].

In [6] the motor and its losses are modelled based on measurement data, whereas the inverter losses are modelled based on manufacturer's data. However, an execution and evaluation of the proposed measurements necessary for the motor loss identification are difficult to automate.

None of the methods in the mentioned contributions can be applied without any knowledge of the drive system. Therefore, this paper pursues a different approach. The basic idea is to obtain the optimal current reference values from test bench measurements only. The execution of the measurements, the evaluation of the data and the parametrization of the inverter can therefore be carried out fully automated.

II. EESM and problem definition

A. Machine

The description of the EESM in the rotating dq-reference frame is derived from [6] and holds for reference quantity invariant transformed space vectors. The stator voltage equations of a rotating electrical machine are given by

$$U_d = R_s I_d + \frac{d\Psi_d}{dt} - \omega \Psi_q \tag{1}$$

$$U_q = R_s I_q + \frac{d\Psi_q}{dt} + \omega \Psi_d, \tag{2}$$

where R_s is the stator resistance and ω represents the electric angular frequency. The relation between the flux linkage components and the current components is defined by the

O. Haala is with the Department of Electrical Engineering, Precision Engineering and Information Technology, Georg Simon Ohm University of Applied Sciences, Nuremberg, Germany, e-mail: HaalaOl40299@th-nuernberg.de.

B. Wagner is with the Department of Electrical Engineering, Precision Engineering and Information Technology, Georg Simon Ohm University of Applied Sciences, Nuremberg, Germany, e-mail: Bernhard.Wagner@th-nuernberg.de.

M. Hofmann is with the Department of Drives and Mechatronics, Fraunhofer Institute for Integrated Systems and Device Technology, Erlangen, Germany, e-mail: Maximilian.Hofmann@iisb.fraunhofer.de.

M. März is with the Department of Power Electronic Systems, Fraunhofer Institute for Integrated Systems and Device Technology, Erlangen, Germany, e-mail: Martin.Maerz@iisb.fraunhofer.de.

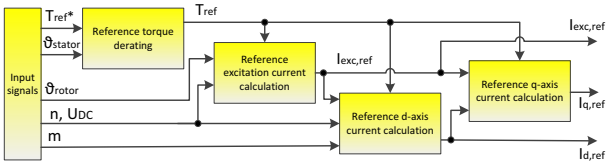

Fig. 1: Current reference calculation

direct inductance L_d, the quadrature inductance L_q and the mutual inductance L_m ((3) and (4)).

$$\Psi_d = L_d I_d + L_m I_{exc} \tag{3}$$

$$\Psi_q = L_q I_q \tag{4}$$

The voltage of the excitation coil can be expressed as

$$U_{exc} = R_{exc} I_{exc} + \frac{d\Psi_{exc}}{dt} \tag{5}$$

with

$$\Psi_{exc} = \frac{3}{2} L_m I_d + L_{exc} I_{exc}, \tag{6}$$

where R_{exc} is the resistance of the exciation coil and L_{exc} its self inductance. The air gap torque

$$T_{ag} = \frac{3}{2} p I_q (L_m I_{exc} + (L_d - L_q) I_d), \tag{7}$$

with the pole pair number p, depends on the three current components I_{exc}, I_d and I_q.

B. Control structure

The FOC of an EESM is known since [9]. The present paper is restricted to the generation of the three optimal current reference values (Fig. 1). In order to consider the maximum admissible stator temperature ϑ_{stator}, the reference torque is reduced from the externally demanded torque value $T_{ref}*$ to T_{ref} at high stator temperatures.

The optimal excitation current reference value depends on the operating point (T_{ref}, rotational speed n and DC link voltage U_{DC}) of the machine. Since the rotor is not actively cooled, special attention has to be paid to the rotor temperature ϑ_{rotor}. For this reason, the excitation current reference value $I_{exc,ref}$ has to be reduced if the rotor becomes too hot.

The optimal direct current reference value is operating point (T_{ref}, n, U_{DC} and $I_{exc,ref}$) dependent as well. The field weakening is performed by reducing the direct current reference value $I_{d,ref}$ iteratively until the modulation index m is adjusted to the desired modulation index m_{max}.

Finally, the quadrature current reference value $I_{q,ref}$ results from the torque request T_{ref} and the reference values $I_{exc,ref}$ and $I_{d,ref}$ (see (7)).

C. Optimization problem (OP)

The determination of the optimal current reference values in steady state can be considered as an optimization problem

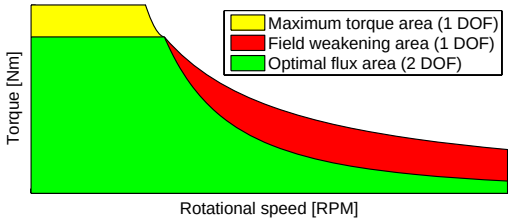

Fig. 2: Operating areas of an EESM

defined by the equation set in (8)

$$\begin{aligned} &\underset{I_{exc},I_d,I_q}{minimize}\ P_l \\ &subject\ to\ T = T_{ref} \\ &\qquad U_{ph} \le U_{ph,max} \\ &\qquad I_{ph} \le I_{ph,max} \\ &\qquad I_{exc} \le I_{exc,max}, \end{aligned} \tag{8}$$

where P_l represents the total losses of the drive system, T is the shaft torque, $U_{ph,max}$ is the maximum phase voltage, $I_{ph,max}$ is the maximum phase current and $I_{exc,max}$ the maximum excitation current of the inverter. U_{ph} and I_{ph} are given by

$$U_{ph} \approx \omega \cdot \Psi = \omega \cdot \sqrt{(L_d I_d + L_m I_{exc})^2 + (L_q I_q)^2} \tag{9}$$

and

$$I_{ph} = \sqrt{I_d^2 + I_q^2}. \tag{10}$$

D. Operating areas

The choice of the current reference values depends on the operating area. If the EESM is controlled optimally, there are mainly three operating areas[1] (Fig. 2). The term base speed range is not used in this contribution because it implies the limitation to a certain rotational speed. Instead, the terms maximum torque area and optimal flux area are used. In the maximum torque area either the phase current or the excitation current is at its maximum. For the system with the basic data provided in appendix A the phase current reaches its maximum first. The field weakening area is characterized by the fact that the phase voltage of the inverter reaches its maximum. On the contrary, in the optimal flux area the stator flux linkage can be chosen optimally because the inverter voltage is sufficient.

III. Analytic Approach

Finding an analytic approach that solves the optimization problem (OP) in (8) is challenging because there is no analytic formula to describe the effect of saturation. Moreover, the target function is the sum of nonlinear functions and therefore difficult to minimize.

However, if two assumptions are made, the OP can be solved by an analytic approach. This approach assumes that the

[1]At very low rotational speeds the inverter cannot provide the maximum phase current because the losses are not distributed equally over one half bridge, and not averaged over time. However, this operating area is very small and therefore neglected in this consideration.

copper losses in the stator and the rotor (see (11)) are the only losses that occur. Moreover, constant inductance values are assumed. The resulting simplified optimization problem (SOP) covers the three operating areas but it is solved separately in each operating area. The solution in each operating area is based on a Lagrange approach.

$$P_{cu} = \frac{3}{2} R_s (I_d^2 + I_q^2) + R_{exc} I_{exc} \tag{11}$$

A. SOP in the optimal flux area

In this operating area the SOP is reduced to

$$\begin{aligned} &\underset{I_{exc}, I_d, I_q}{minimize}\ P_{cu} \\ &subject\ to\ T = T_{ref} \end{aligned} \tag{12}$$

and the Lagrange approach is

$$\Lambda = P_{cu} + \lambda (T - T_{ref}), \tag{13}$$

with the Lagrange multiplier λ. If the partial derivatives $\frac{\partial \Lambda}{\partial I_{exc}}, \frac{\partial \Lambda}{\partial I_d}, \frac{\partial \Lambda}{\partial I_q}$ are set to zero, the elimination of λ yields in the two equations

$$I_{q,opt}^2 - I_{d,opt}^2 - I_{d,opt} \frac{L_{m0} I_{exc,opt}}{L_{d0} - L_{q0}} = 0 \tag{14}$$

and

$$I_{d,opt} = I_{exc,opt} \cdot c_1 \tag{15}$$

with

$$c_1 = \frac{2 R_{exc} (L_{d0} - L_{q0})}{3 R_s L_{m0}}, \tag{16}$$

where the subscript zero indicates an unsaturated value. Equation (14) and (15) represent the optimality condition for the two remaining DOF. The optimal current reference values

$$I_{exc,opt} = \sqrt{\frac{2\ T_{ref} \sqrt{\frac{3 R_s}{3 R_s c_1^2 + 2 R_{exc}}}}{3p(L_{m0} + c_1 (L_{d0} - L_{q0}))}} \tag{17}$$

$$I_{d,opt} = c_1 \cdot I_{exc,opt}, \tag{18}$$

and

$$I_{q,opt} = \frac{2\ T_{ref}}{3p(L_{m0} I_{exc,opt} + (L_{d0} - L_{q0}) I_{d,opt})} \tag{19}$$

in this operating area result from solving (7), (14) and (15).

B. SOP in the field weakening area

In this operating area the phase voltage of the inverter reaches its maximum and therefore the SOP reads as follows:

$$\begin{aligned} &\underset{I_{exc}, I_d, I_q}{minimize}\ P_{cu} \\ &subject\ to\ T_{mot} = T_{ref} \\ &\qquad\qquad U_{ph} = U_{ph,max} \end{aligned} \tag{20}$$

The Lagrange approach

$$\Lambda = P_{cu} + \lambda_1 (T - T_{ref}) + \lambda_2 (U_{ph} - U_{ph,max}) \tag{21}$$

leads to the optimality condition (22) for the remaining DOF in this operating area.

$$I_{q,opt} = \pm \sqrt{\frac{(3 R_s L_{m0} I_{d,opt} - 2 R_{exc} L_{d0} I_{exc,opt}) \Psi_1 \Psi_2}{3 R_s L_{m0} (L_{q0}^2 I_{d,opt} + \Delta L \Psi_2 - L_{d0} \Psi_1) - 2 R_{exc} L_{q0}^2 \Delta L I_{exc,opt}}} \tag{22}$$

with the substitution variables

$$\begin{aligned} \Delta L &= L_{d0} - L_{q0} \\ \Psi_1 &= L_{m0} I_{exc,opt} + L_{d0} I_{d,opt} \\ \Psi_2 &= L_{m0} I_{exc,opt} + \Delta L I_{d,opt} \end{aligned}$$

However, the resulting system of equations ((7), (9) and (22)) cannot be solved for $I_{exc,opt}$, $I_{d,opt}$ and $I_{q,opt}$ in a fully analytic way because the resulting polynomials exceed the fourth degree. For this reason, the system of equations was solved iteratively by the Gauss-Newton algorithm.

C. SOP in the maximum torque area

In this operating area the phase current of the inverter reaches its maximum and therefore the SOP is reduced to

$$\begin{aligned} &\underset{I_{exc}, I_d, I_q}{minimize}\ P_{cu} \\ &subject\ to\ T_{mot} = T_{ref} \\ &\qquad\qquad I_{ph} = I_{ph,max}. \end{aligned} \tag{23}$$

The optimality condition for the remaining DOF

$$I_{q,opt} = \pm \sqrt{I_{d,opt} (I_{d,opt} + I_{exc,opt} \frac{L_{m0}}{L_{d0} - L_{q0}})} \tag{24}$$

results from the Lagrange approach

$$\Lambda = P_{cu} + \lambda_1 (T - T_{ref}) + \lambda_2 (I_{ph} - I_{ph,max}). \tag{25}$$

Like in subsection III-B, the system of equations ((7), (10) and (24)) cannot be solved fully analytically and is therefore solved iteratively by the Gauss-Newton algorithm.

D. Results

The optimal current reference values (Fig. 3, 4 and 5) are calculated with the parameters in Tab. I. In this subsection the current limitations of the inverter (Tab. II) were reduced to $I_{ph,max} = 215\ A$ and $I_{exc,max} = 9.1\ A$ in order to consider the maximum shaft torque ($T_{max} = 200\ Nm$).

IV. Numeric approach

A. Basic idea

The basic idea of this numeric approach is to overcome the assumptions made in section III. For this reason, the functions in (8) are identified by test bench measurements.

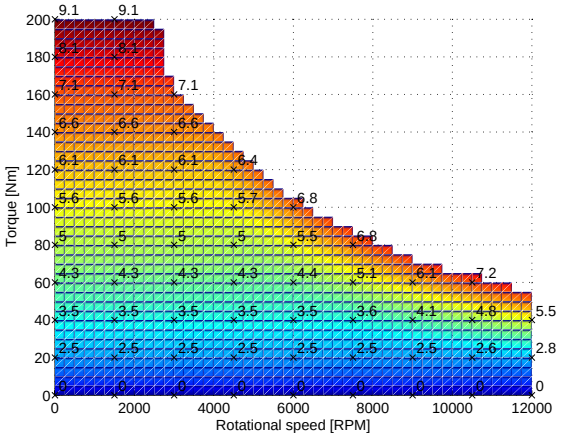

Fig. 3: Optimal excitation current

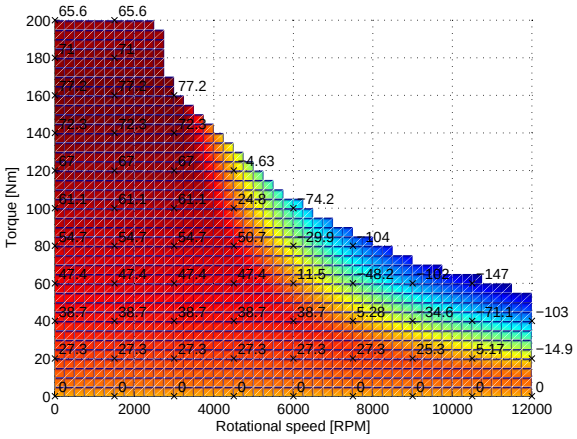

Fig. 4: Optimal d-current component

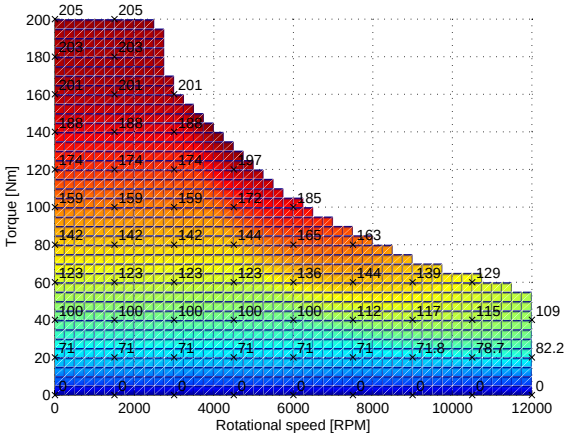

Fig. 5: Optimal q-current component

B. Test bench setup

The electric drive is fed by a constant DC voltage source and a constant rotational speed is adjusted by a test bench machine

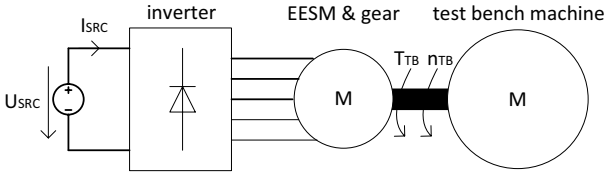

Fig. 6: Test bench setup

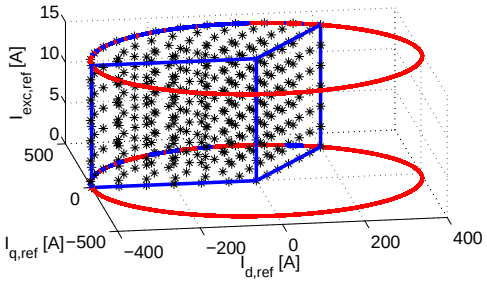

Fig. 7: Set of current reference values

(Fig. 6). The inverter control unit provides a CAN/CCP interface which is used to set the three current reference values and to read internal signals of the inverter. The most important measurement values are the electric quantities U_{SRC} and I_{SRC} measured at the electric energy source and the mechanic quantities n_{TB} and T_{TB} measured at the test bench machine. These values are provided by a CAN interface of the test bench.

C. Measurement

In the proposed measurement a total number of $7^3 = 343$ operating points are acquired (black stars in Fig. 7). If this measurement is fully automated, it lasts approx. 90 minutes only. The red circles result from the maximum admissible inverter phase current. The space between the two red circles represents the set of feasible operating points at rotational speeds below the rated rotational speed n_R. The measurement of positive quadrature currents is sufficient, because $I_{q,opt}(T_{Ref}) \approx -I_{q,opt}(-T_{Ref})$. In spite of the fact that the reluctance torque of an EESM with salient poles ($L_{d0} > L_{q0}$) is positive, positive direct currents should be avoided in order to prevent the immoderate saturation of the main inductance. For this reason, only operating points with a comparatively small positive direct current are measured. However, the full range of negative direct currents has to be measured to cover the field weakening area completely.

All measurements are performed at a constant rotational speed and a constant source voltage. In order to ensure an approx. constant stator and rotor temperature the chronological order of the operating points was adapted and the drive was temperature conditioned.

D. Evaluation

Before the measurement data are evaluated an interpolation with a high resolution is performed for each measured quantity

$Q = f(I_{exc}, I_d, I_q)$.

The shaft torque is obtained from the measured torque by considering the gear transmission ratio and a constant (warm) gear efficiency of 96%. The torque function

$$T = f_T(I_{exc}, I_d, I_q) \Rightarrow I_{q,ref} = f_{Iq}(T_{ref}, I_{exc,ref}, I_{d,ref}) \quad (26)$$

is necessary to satisfy the torque constraint in (8) and is used to calculate f_{Iq}, which is necessary for the quadrature current reference calculation, by a numeric transformation.

The total losses of the electric drive are calculated by

$$P_l = |U_{SRC} \cdot I_{SRC} - T_{TB} \cdot 2\pi n_{TB}| \quad (27)$$

in each operating point and represent the target function

$$P_l = f_{P*}(I_{exc}, I_d, I_q)\Big|_{n,U_{SRC}} \overset{f_{Iq}}{=} f_P(T, I_{exc}, I_d)\Big|_{n,U_{SRC}}, \quad (28)$$

which is valid at a certain rotational speed and a certain supply voltage. The measurements in this paper were performed at a supply voltage of 400 V. However, the optimal current reference values can be identified for various supply voltages. For this reason, the dependency on the supply voltage is omitted in further considerations. Based on two measured target functions $f_{P1} = f_P\big|_{n=n_1=470\ RPM}$ and $f_{P2} = f_P\big|_{n=n_2=3760\ RPM}$ the dependency of the target function on the rotational speed was modelled as a piecewise defined function.

$$f_P\Big|_n = \begin{cases} m_{f_P} \cdot (n - n_1) + f_{P1} & if \quad n \in [0, n_R] \\ m_{f_P} \cdot (n_R - n_1) + f_{P1} & if \quad n \in]n_R, n_{max}] \end{cases} \quad (29)$$

with $m_{f_P} = (f_{P2} - f_{P1})/(n_2 - n_1)$

Especially at high rotational speeds the approximation of this function will become less accurate because the stray losses will increase. Therefore, the system efficiency might not be optimal anymore but still very close to the optimum. From the representation of P_l in (28) it can be concluded that there is at a certain rotational speed for each torque value (at least) one combination of I_{exc} and I_d that minimizes P_l. The optimal current reference values are obtained by a numeric minimization of P_l (Fig. 8). Since the set of measured operating points already considers the current constraint functions in (8), they do not need to be considered in the minimization anymore. Therefore, the optimal current reference values in the optimal flux and the maximum torque area result immediately from this minimization.

However, in the field weakening area the set of feasible operating points is limited due to the voltage inequality constraint. The phase voltage function at an arbitrary rotational speed

$$U_{ph} = f_U(I_{exc}, I_d, I_q)\Big|_n \quad (30)$$

is obtained easily from a phase voltage function at a certain rotational speed ($\in \ ]0, n_R]$) due to the proportionality in (9). Therefore, for each rotational speed each operating point that violates the voltage constraint has to be rejected. The loss minimization is performed amongst the remaining set of operating points.

If the optimal excitation current cannot be applied due to a high rotor temperature or a demand for high dynamics, there will be still one DOF left in the optimal flux area. Then the optimization between the direct and the quadrature current is performed for each excitation current reference value.

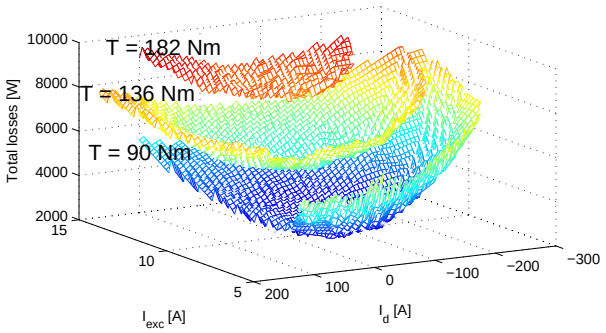

Fig. 8: Cross sections of the target function at $n = 2350\ RPM$

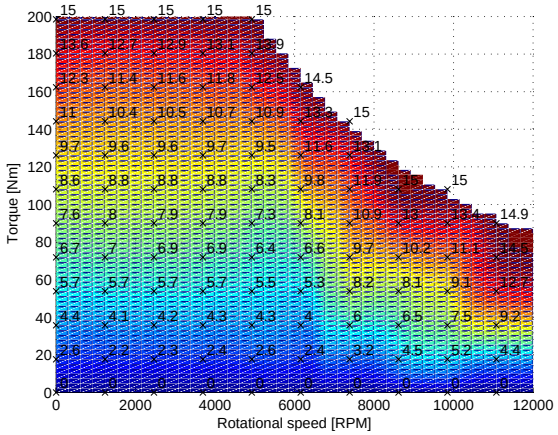

Fig. 9: Optimal excitation current at $U_{SRC} = 400\ V$

E. Results

At small rotational speeds and small torque values the results are in good agreement with the analytic solution in section III-D. At higher torque values, however, owing to highly saturation dependent inductance values the optimal excitation and quadrature current values in Fig. 9 and Fig. 11 are considerably above the current values in Fig. 3 and Fig. 5. Almost over the whole operating area, the optimal direct current in Fig. 10 tends to be smaller than in Fig. 4. Especially in the maximum torque area the direct current is used to reduce the flux density in the magnetic circuit.

Figure 12 shows how the direct current reference value is generated in the maximum torque and the optimal flux area if the excitation current reference value is changed from its optimal value. If the changed reference value is above the absolute minimum (transition between the white and the coloured area), the phase current is not maximal and therefore one DOF is remaining. The optimal direct current reference value in each operating point is indicated by the colour.

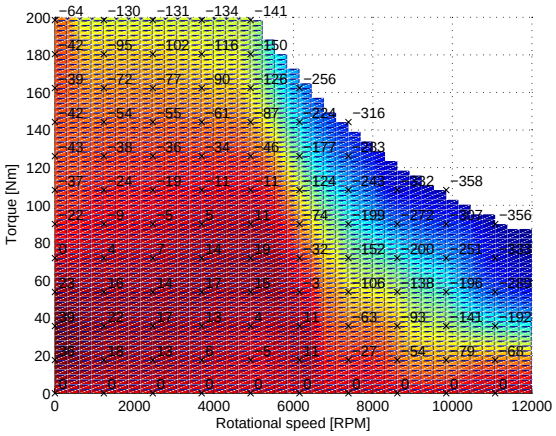

Fig. 10: Optimal d-current component at $U_{SRC} = 400\ V$

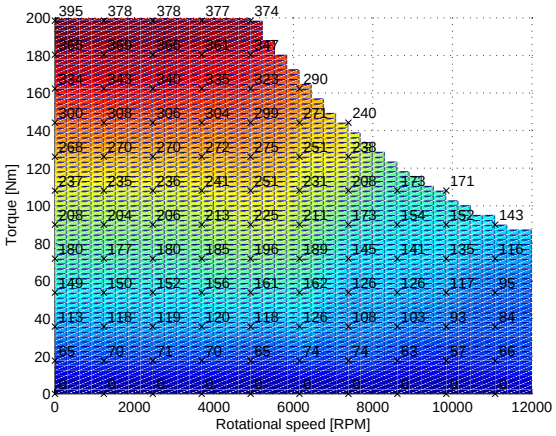

Fig. 11: Optimal q-current component at $U_{SRC} = 400\ V$

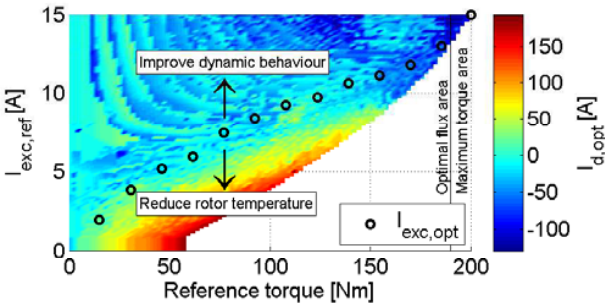

Fig. 12: Optimal direct current component at $n = 2350\ RPM$, $U_{SRC} = 400\ V$

V. Comparison with Kanelis ([8])

If the current reference values are chosen according to [8], there will only be two operating areas which are separated by a rated rotational speed n_{R*}. Below this rotational speed the nominal stator flux linkage is set (constant flux area), whereas above this speed the nominal stator flux linkage is reduced by the factor $\frac{n_{R*}}{n}$ (field weakening area). In both operating areas the condition $\cos(\varphi) = 1$ is satisfied. From these conditions and a saturation dependent machine model the resultant current reference values are calculated offline. Advantages of this control strategy are the good utilization of both the magnetic circuit and the inverter.

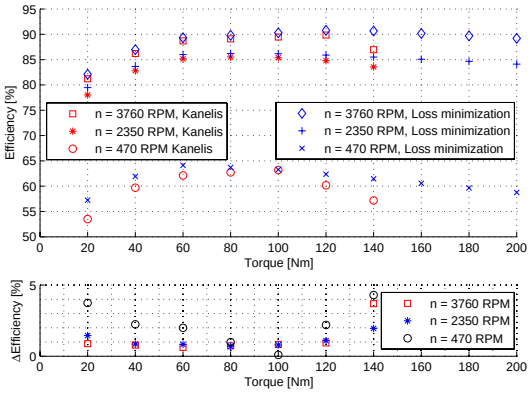

Fig. 13: Comparison between the system efficiencies obtained by [8] and section IV

In comparison to the control strategy in section IV there are mainly two differences. Since the stator flux linkage is limited to the nominal flux linkage, the maximum achievable torque in the constant flux area is smaller (150 Nm instead of 200 Nm). Based on (29) the system efficiencies of both control strategies were determined (see Fig. 13).

Since the total losses of the drive system in the field weakening area are based on an extrapolation, the comparison of the system efficiencies is limited to the constant flux area. In this operating area the proposed method shows a better calculated system efficiency than the system efficiency that results from the control strategy in [8].

VI. Conclusion

This article presents a novel method to determine the optimal current reference values of an EESM in automotive traction drive applications. The three operating areas of the EESM were derived from the definition of the optimization problem in (8). After an analytic preliminary consideration a numeric approach was chosen to solve the OP offline. The solution represents those current reference values which are optimal in terms of a system efficiency maximization. Moreover, the demand for a high dynamic behaviour and the protection against too high rotor temperatures was addressed in both the control structure and the optimization. The data which are required by the proposed method were obtained by test bench measurements only. The advantages of the proposed method are a high system efficiency, a high suitability for an automated calibration of the inverter control unit and the applicability on a drive system with unknown parameters.

The efficiency of the drive system can be further improved if the target function is modelled in more detail. For this purpose

measurements at lower source voltages and measurements at high rotational speeds are recommended.

APPENDIX A
SYSTEM PARAMETERS

TABLE I: EESM parameters

Symbol	Quantity	Value
T_{max}	Maximum torque	200 Nm
n_{max}	Maximum rotational speed	12000 RPM
n_R	Rated rotational speed	4750 RPM
	(with the inverter from Tab. II)	
p	Number of pole pairs	4
R_s	Stator resistance (at 20° C)	7.1 $m\Omega$
R_{exc}	Excitation resistance (at 20° C)	7.3 Ω
L_{d0}	Direct inductance (unsaturated)	615 μH
L_{q0}	Quadrature inductance (unsaturated)	360 μH
L_{m0}	Mutual inductance (unsaturated)	16 mH
L_{exc0}	Excitation inductance (unsaturated)	0.8 H
Ψ_N	Nominal stator flux linkage	80 mVs

TABLE II: Inverter parameters

Symbol	Quantity	Value
$U_{DC,nom}$	Nominal DC link voltage	400 V
$I_{ph,max}$	Maximum phase current (space vector)	400 A
$I_{exc,max}$	Maximum excitation current	15 A
$U_{ph,max}$	Maximum phase voltage (space vector)	231 V
f_T	Switching frequency	10 kHz

REFERENCES

[1] J. Santiago, H. Bernhoff, B. Ekergard, S. Eriksson, S. Ferhatovic, R. Waters, M. Leijon, *Electrical Motor Drivelines in Commercial All-Electric Vehicles: A Review*, IEEE Transactions on vehicular technology, vol. 61, no. 2, February 2012.
[2] M. Märgner, W. Hackmann, *Control challenges of an externally excited synchronous machine in an automotive traction drive application*, Emobility - Electrical Power Train, November 2010.
[3] M. Niemelä, *Position sensorless electrically excited synchronous motor drive for an industrial use based on direct flux linkage and torque control*, PhD thesis, Lappeenranta University of Technology, Finnland, 1999.
[4] I. Boldea, G. Andreescu, C. Rossi, A. Pilati, D. Casadei *Active Flux Based Motion-Sensorless Vector Control of DC-Excited Synchronous Machines*, Energy Conversion Congress and Exposition, September 2009.
[5] A. Girardin, G. Friedrich, *Optimal control for a Wound Rotor Synchronous starter generator*, Industry Applications Conference, October 2006.
[6] R. Grune, *Verlustoptimaler Betrieb einer elektrisch erregten Synchronmaschine für den Einsatz in Elektrofahrzeugen*, PhD thesis, Technische Universität Berlin, Germany, 2012.
[7] H. Karmaker, *Stray losses in large synchronous machines*, IEEE Transactions on Energy Conversion, vol. 7. no. 1, March 1992.
[8] K. Kanelis, *Die feldorientierte Kennliniensteuerung der stromerregten Synchronmaschine* , PhD thesis, Universität der Bundeswehr München, Germany, 1994.
[9] K. H. Bayer, H. Waldmann, M. Weibelzahl *Die Transvector-Regelung für den feldorientierten Betrieb einer Synchronmaschine*, Siemens Zeitschrift, Heft 10, 1972.

Oliver Haala (1988) received his B.Eng. in Electrical Engineering from Georg Simon Ohm University of Applied Sciences, Nuremberg in 2012. He continued studying at Georg Simon Ohm University of Applied Sciences and is presently working towards the M.Sc. in Applied Research.

Dr.-Ing. Bernhard Wagner (1965) received his Diploma Degree at the University of Erlangen in 1992 and PhD (Dr.-Ing.) in 1999 in the field of iterative learning control. Since 2007 he is Professor for Control Systems at the Ohm-University Nuremberg. Field of research is control of electric drives and traction systems.

Dr.-Ing. Maximilian Hofmann (1981) is working since 2007 at the Fraunhofer IISB in Erlangen in the department Power Electronic Systems. Since 2011 he is leading the group Drives and Mechatronics in this department dealing with electric drives and power electronics for HEV and BEV. The topic of his PhD thesis was the mechatronic integration of inverter power electronics into electric machines.

Dr.-Ing. Martin März (1962) studied at the University of Erlangen-Nuremberg specializing in high frequency engineering. After his PhD on laser topics, he started his career in the semiconductor division of the Siemens AG, later Infineon AG. Since 2000 he is working for the Fraunhofer "Institute of Integrated Systems and Device Technology" in Erlangen and Nuremberg (Germany) as head of the power electronics system department, since 2012 as the deputy director of the IISB. He is working on system integration of power electronics, thermal management, and on new technologies for power density, efficiency, and reliability improvements.